Scientific Research Publishing

Open Journal of Civil Engineering, 2024, 14, 196-213
https://www.scirp.org/journal/ojce
ISSN Online: 2164-3172
ISSN Print: 2164-3164

The Performance of Small Diameter Aluminum Light Support Structures Containing Handholes under Cyclic Fatigue

Cameron R. Rusnak[1*], Aya Al-Hamami[1], Craig C. Menzemer[2]

[1]Department of Science, Technology, and Mathematics, Lincoln University of Missouri, Jefferson, Missouri, USA
[2]Auburn Science and Engineering Center, Department of Civil Engineering, The University of Akron, Akron, Ohio, USA
Email: *RusnakC@lincolnu.edu, aya.al-hamami116@my.lincolnu.edu, ccmenze@uakron.edu

How to cite this paper: Rusnak, C.R., Al-Hamami, A. and Menzemer, C.C. (2024) The Performance of Small Diameter Aluminum Light Support Structures Containing Handholes under Cyclic Fatigue. *Open Journal of Civil Engineering*, **14**, 196-213.
https://doi.org/10.4236/ojce.2024.142010

Received: May 30, 2024
Accepted: June 25, 2024
Published: June 28, 2024

Abstract

Aluminum light poles play a pivotal role in modern infrastructure, ensuring proper illumination along highways and in populated areas during nighttime. These poles typically feature handholes near their bases, providing access to electrical wiring for installation and maintenance. While essential for functionality, these handholes introduce a vulnerability to the overall structure, making them a potential failure point. Although prior research and analyses on aluminum light poles have been conducted, the behavior of smaller diameter poles containing handholes remains unexplored. Recognizing this need, a research team at the University of Akron undertook a comprehensive experimental program involving aluminum light poles with handholes containing welded inserts in order to gain a better understanding of their fatigue life, mechanical behavior, and failure mechanisms. The research involved testing seven large-scale aluminum light poles each 8-inch diameter, with two separate handholes. These handholes included a reinforcement that was welded to the poles. Finite Element Analysis (FEA), statistical analysis, and comparison analysis with their large counterparts (10-inch diameter) were used to augment the experimental results. The results revealed two distinct failure modes: progressive crack propagation leading to ultimate failure, and rupture of the pole near the weld initiation/termination site around the handhole. The comparison analysis indicated that the 8-inch diameter specimens exhibited an average fatigue life exceeding that of their 10-inch counterparts by an average of 30.7%. The experimental results were plotted alongside the fatigue detail classifications outlined in the Aluminum Design Manual (ADM), enhancing understanding of the fatigue detail category of the respective poles/handholes.

Keywords

Light Pole, Handhole, Cyclic Fatigue, Fatigue Analysis, Finite Element Analysis, Statistical Analysis

1. Introduction

Light poles are essential to modern infrastructure as they provide safety and security for those driving on roadways, parking lots, commercial centers, industrial facilities, and to those walking on nearby sidewalks. When spaced appropriately, they can eliminate dark spots and alert cars and pedestrians to potential hazards [1] [2]. A critical aspect of light pole design and construction is the electrical access handhole placed near the base of the pole. These holes typically contain a reinforcement that is welded into position [3]. These handholes allow for necessary access to the electrical wiring system for both installation and maintenance purposes. However, while integral to the functionality of the light pole, these handholes present a vulnerability within the system and may represent a potential failure location. Proper inspection, maintenance and replacement of light poles can significantly reduce the risk associated with unexpected collapses and, most importantly, safeguard against the loss of human life.

Throughout history, wind-induced fatigue cracking has been identified as a significant factor leading to structural failure and collapse of light poles [4]. Notable incidents include the failure of a light pole on the Western Link Elevated Road in September 2003, causing disruption to northbound traffic. Additionally, in June 2004, a light pole near the crest of the Bolte Bridge experienced a similar failure [5]. In March 2009, during a girls' soccer game at Hays High School in Buda, Texas, a light pole surrounding the stadium collapsed onto the roof of an adjacent gymnasium [6] [7]. It has been reordered that steel light poles manufactured by Whtico Co. LLP have fallen 11 times between 2000-2010 [8]. In 2014, light pole structures in a large public parking lot in Kansas failed due to extreme wind conditions, with subsequent investigations revealing propagating fatigue cracks near critical locations [9]. Tsai *et al.* discussed a research article detailing the collapse of a high-mast light pole along I-29 near Sioux City in 2003, early in its service life, among other failures [10]. Koob's article on high mast towers and pole luminaries highlighted a case where a 140-foot-tall tower failed, with inspection revealing cracking in the handhole, as depicted in "**Figure 1**" [11].

Numerous studies have explored the complexities surrounding light poles and their fatigue life. Roy *et al.* [12] examined cost-effective connection details for highway sign, luminaire, and traffic signal structures. Their study involved testing 80 full-sized galvanized specimens of various support structures under fatigue, coupled with Finite Element Analysis, leading to proposed specification revisions for AASHTO standards. Consolazio *et al.* [13] conducted a three-month

monitoring study of a Variable Message Sign (VHS) to determine equivalent static pressures for fatigue loads, informing future sign support structure design. Oterkus *et al.* [14] performed stress analysis on composite cylindrical shells with elliptical cutouts, establishing design criteria for laminated composite shells. The University of Akron has conducted multiple investigations on aluminum light poles and their fatigue life. Azzam [15] studied the fatigue behavior of welded aluminum light poles, focusing on socket connections. Daneshkhah *et al.* [16] examined reinforced welded handholes in aluminum light poles, developing S-N curves and analyzing mechanical behavior. Schlater's master's thesis [17] investigated the fatigue behavior of reinforced electrical access handholes on 10-inch diameter specimens, available in the "OhioLink" library. Rusnak *et al.* conducted extensive research on aluminum light poles and associated handholes, covering topics such as flush-insert-design handholes [18], open-unreinforced handholes [19], geometry changes [20], and fracture mechanics analysis [21]. Rusnak's master's thesis and doctoral dissertation [22] [23], available in the "OhioLink" library. Rusnak's master's thesis focused on the fatigue life of smaller-sized aluminum light poles. His dissertation further explored the nuances of various aspects of a handhole present in aluminum light poles. This included examining a flush design, a nonreinforcement design, and changes in the geometry of the insert design. Each aspect was analyzed using Finite Element Analysis and Fracture Mechanics Analysis.

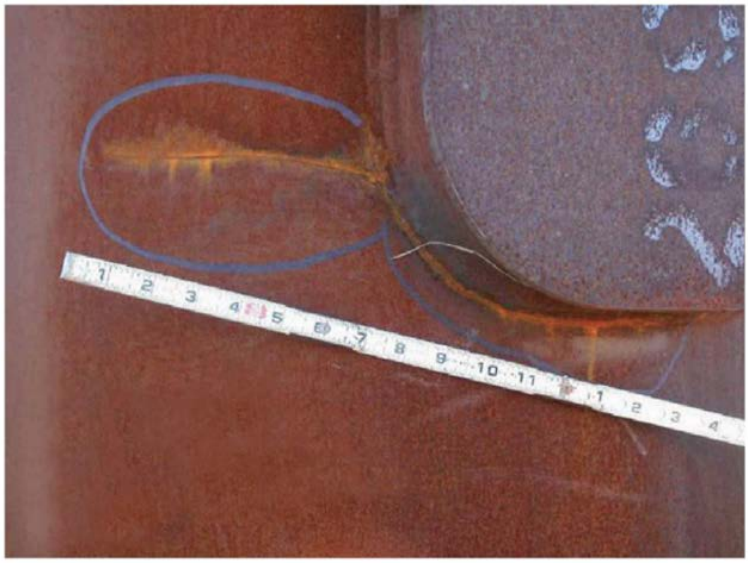

Figure 1. Cracking around handhole in high mast tower [10].

Hoeppner *et al.* [24] explored the prediction of component life through the application of fatigue crack growth, providing examples of generated forms of fatigue-crack growth laws. Their study aimed to demonstrate how fatigue-crack growth concepts can be applied to predict life, enhance reliability, select appropriate materials, improve design, and establish inspection criteria. Fatemi *et al*

[25] conducted a study on cumulative fatigue damage and life prediction for homogenous materials. Carpinteri *et al.* [26] investigated the size effect of fatigue life in metals. Their findings were in line with previous research on the subject, indicating that as the size of a general specimen increases, the fatigue life decreases.

Statistical analysis is a powerful tool that helps researchers examine and understand data across various fields such as engineering, science, business, healthcare, and the social sciences. Its primary focus is on gathering, sorting, studying, and interpreting data to reveal hidden patterns, trends, and draw connections [27]. The primary objective of statistical analysis is to unravel complex data sets using mathematical and computational methods. This process assists researchers and analysts in drawing conclusions, testing hypotheses, and making predictions grounded in empirical evidence [28] [29]. Statistical analysis encompasses a wide array of methods and techniques. Descriptive statistics serve as summaries, akin to snapshots, that highlight key aspects of a dataset by revealing the average or most frequent values. Inferential statistics enable us to make estimations or forecasts about a broader population using a smaller sample.

The research presented in this paper is a part of a comprehensive analysis of aluminum light poles conducted at the University of Akron [15]-[21]. The current study begins by introducing the experimental setup utilized in the laboratory to test 8-inch diameter aluminum light poles with cast handholes welded into position. Subsequently, the cyclic loading protocol is outlined. The investigation examines the fatigue life and mechanical behavior of the aluminum light poles concerning their capacity. Fatigue life of the specimens was plotted as S-N curves and compared to the standard details outlined in the Aluminum Design Manual [30] in order to determine the fatigue detail category of the handholes tested. Additionally, Finite Element Analysis (FEA), statistical analysis and comparison to larger size poles were conducted alongside the laboratory experiments to enhance understanding of the behavior and fatigue life of the aluminum light poles.

2. Experimental Program and Finite Element Models of the Aluminum Light Support Structures

2.1. Experimental Setup and Loading Protocol

The present aluminum light support structure study encompassed a total of seven (7) individual large-scale tests, with an emphasis on the handholes that contained a reinforcement welded into place. The specimens were 8-inch in diameter with a wall thickness of 0.25-in and contained 2 handholes. The body of the pole measured 12-feet (144-inch) in length, with the center of each handhole positioned 54-inch from each end of the pole respectively. The industry-standard oval reinforcement welded into the handholes measured 4-inch × 6-inch, with the major dimension along the vertical/longitudinal axis [3]. Handholes were welded into place using Gas Metal Arc Welding (GMAW) [31] prior to delivery

to the University of Akron. "Figure 2" depicts a sample laboratory image of the handhole reinforcement welded into the light pole.

Figure 2. Sample image of handhole reinforcement welded into the pole.

Each specimen was positioned on two (2) separate rollers, approximately 6 inches from each end of the pole respectively. A spreader bar, 100 inches in length with steel rollers attached 8 inches from each end, was used to facilitate four-point bending. This spreader bar was placed on the specimen with the rollers 30 inches from each end of the pole respectively. Loaded was applied using a 55-kip servo-hydraulic actuator powered by an MTS STS controller system, attached to the center of the spreader bar. Comprehensive details regarding the material properties of pole/tube, cast insert, and weldment are available in the following databases: Pole [32], Cast Insert [33], and Weld [34]. All materials underwent heat treatment, increasing the tempter to T6 [35] prior to delivery to the University of Akron. "Figure 3" depicts the test setup, and "Figure 4" depicts a photograph from the laboratory. "Figure 5" depicts a simple sketch of the pole, with reference to a clock around the handholes and handhole labels for each specimen.

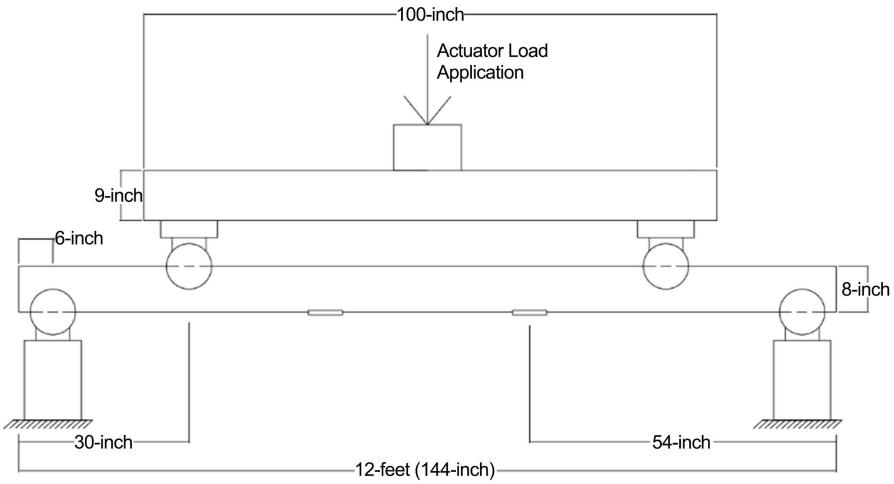

Figure 3. Test setup.

Figure 4. Laboratory photo of test setup.

Figure 5. Clock orientation around a handhole.

In real-world scenarios, wind loading on structures occurs at irregular intervals and can be characterized as a variable amplitude. However, conducting laboratory testing with variable amplitude loading can be challenging. To address this issue and bridge the gap to a constant amplitude loading protocol, the application of Miners Rule [36] [37] [38] and the Rainflow counting algorithm [39] is appropriate. These methods enable the use of a constant amplitude loading protocol when analyzing structures subjected to variable amplitude loading. As a result, cyclic loading with a constant amplitude was chosen as the appropriate loading protocol for testing in this study. This approach allows for a more controlled and manageable testing environment while still capturing the essential fatigue behavior of the aluminum light support structures under variable loading conditions experienced in the field.

In the study, various stress ranges were chosen to undergo cyclic loading at a constant amplitude. The chosen stress ranges were selected in order to facilitate a straightforward comparison with the ADM [30]. "**Table 1**" provides details of the tested stress ranges, corresponding specimen numbers, and cycle rates. Larger stress ranges were cycled at 1 hertz, while smaller stress ranges were cycled at 2 hertz. This approach aimed to reduce the total testing time for smaller stress ranges. The MTS STS software's internal counter was utilized to monitor the number of cycles completed during testing and a maximum displacement for the actuator was set for each experiment so that when failure occurred, the

actuator shut down. Testing was conducted around the clock until failure was achieved.

Table 1. Constant amplitude cyclic stress ranges.

Stress Range (Mpa)	Specimen #	Rate (HZ)
17.86	6	2
24.75	5	2
31.03	4	2
38.20	3	1
44.33	2	1
50.95	1	1
62.68	7	1

Testing was concluded when any of the following conditions were met:

- Cracking of the handhole resulting in detail failure;
- Structure failure of the pole; or
- Cycle count reaching 20,000,000 cycles passed, equating to no failure in the specimen.

It is essential to recognize that the light poles contained two (2) separate handholes. In the event of failure in one handhole, a moment reinforcement clamp was placed around the failed handhole to enable testing to continue. This allowed for more data points to be collected from a single specimen.

2.2. Finite Element, Statistical and Comparison Analyses

Finite Element Analysis (FEA) was utilized to enhance the understanding of the reinforced handholes under bending. FEA models, built at a 1:1 scale, represented the four-point bending specimens. Geometric models were constructed using SolidWorks and imported into the FEA software, ABAQUS. ABAQUS was chosen for its capability to accurately assess stress concentrations around the handholes. The FEA meshing utilized a "shell" model with a global element size set to 0.5. The reinforcement locations in the FEA model mirrored those in laboratory experiments and were constrained in all directions. A constant force of 7 N was applied at the same location where loading occurred in the laboratory setup. These loading and constraint configurations align with previous studies by Daneshkhah, Schlatter, and Rusnak [15]-[20]. "**Figure 6**" depicts the FEA model within ABAQUS.

The research team conducted a power regression statistical analysis on the 8-inch and 10-inch diameter (from Schlatter *et al.* [16]) specimens. The S-N data was the focal point of the statistical analysis. The analysis procedure employed experimental data to determine the trend line, which was subsequently utilized to extrapolate the data into untested stress ranges. Two (2) separate analyses were performed encompassing the 8-inch specimens and the 10-inch specimens.

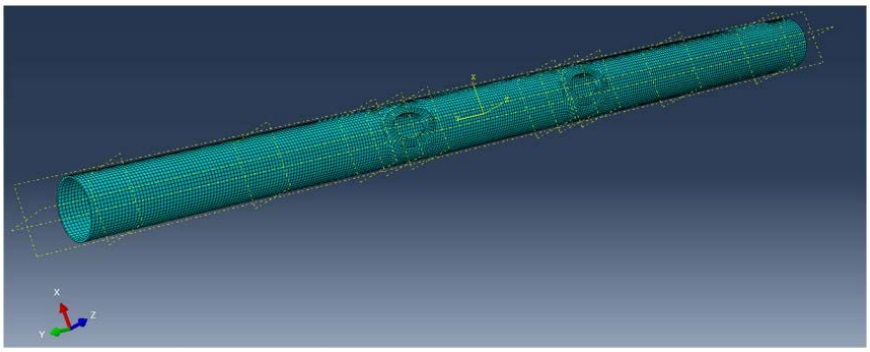

Figure 6. Finite element model.

A comparison analysis was conducted to assess the fatigue life of the 8-inch diameter specimens in relation to 10-inch diameter specimens, focusing on the S-N curves of each study. The reference study for comparison was conducted by Schlatter at the University of Akron [16]. Additional FEA models were developed with loading conditions comparable to Schlatter's study to investigate the impact of size on stress concentrations.

3. Experimental and Analytical Results of the Aluminum Light Support Structures

3.1. Experimental Behavior and Physical Damages

During experimental testing, two distinct failure modes were identified. The first, referred to as "Failure Mode 1," involved fatigue cracking originating at the throat of the weld. This cracking typically began at either the 3 o'clock or 9 o'clock position of the welded handhole, gradually extending along the weldment until reaching a critical point where the crack penetrated into the casting, leading to ultimate failure. In some instances, the pole fractured at either the 3 o'clock or 9 o'clock position following crack propagation. The second failure mode, referred to as "Failure Mode 2," occurred at the base of the handhole, specifically around the 6 o'clock position, coinciding with the location of weld initiation/termination. In this mode, the pole ruptured at the identified location. "**Figures 7-11**" depict images of the observed damage and "**Table 2**" provides comprehensive details of the damage observed, along with corresponding figures.

Table 2. List of observed damage.

Failure Mode	Observations/Damage Description
Failure Mode 1	Fatigue crack initiating at either the 3 or 9 o'clock position after propagation and failure. In this case, final failure/fracture occurred in both the casting and pole ("**Figure 7**" and "**Figure 8**"). Fatigue crack initiating at either the 3 or 9 o'clock position after propagation and failure. In this case, final failure/fracture occurred in the pole and no cracking was observed in the casting ("**Figure 9**" and "**Figure 10**").
Failure Mode 2	Fracture of the pole at approximately the 6 o'clock position corresponding with the weld initiation/termination location ("**Figure 11**").

Figure 7. Failure Mode 1 longitudinal fatigue crack and failure of the casting and Pole Case 1.

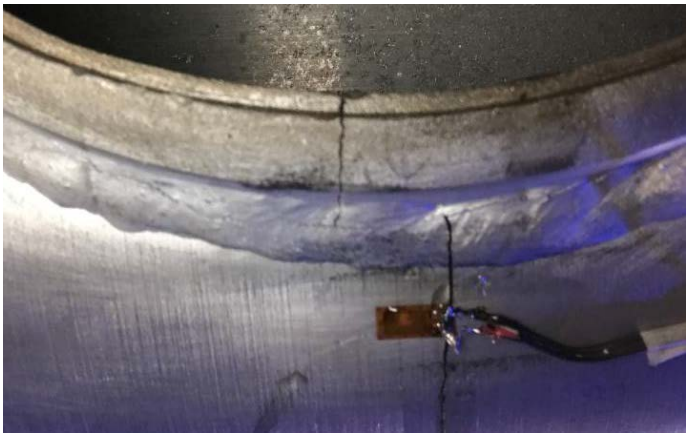

Figure 8. Failure Mode 1 longitudinal fatigue crack and failure of the casting and Pole Case 2.

Figure 9. Mode 1 longitudinal fatigue crack and failure of the Pole Case 1.

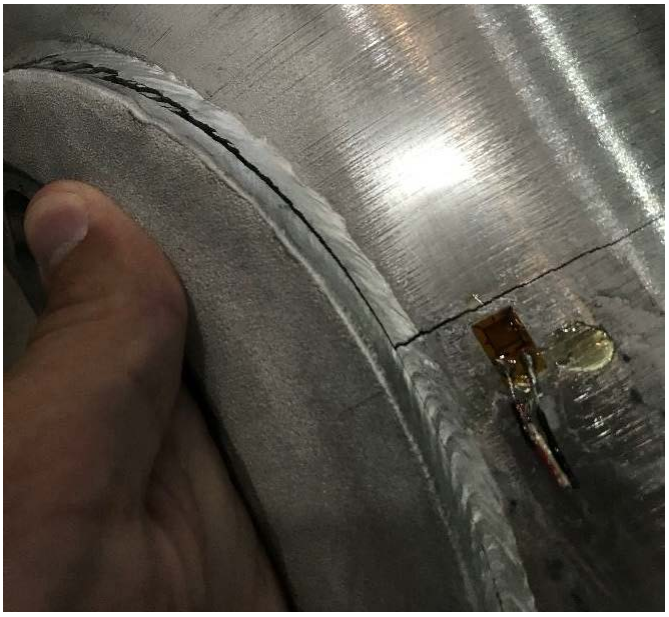

Figure 10. Mode 1 longitudinal fatigue crack and failure of the Pole Case 2.

Figure 11. Failure Mode 2 pole rupture.

During testing, twelve (12) handholes experienced one of two failure modes, resulting in the failure of six (6) out of seven (7) poles tested. Among these, two (2) handholes remained intact due to the low stress range applied during cyclic testing. The test was automatically terminated by the MTS STS software when the internal cycle counter surpassed 20,000,000 cycles. "**Table 3**" presents the experimental outcomes, arranged in ascending order based on stress range, alongside corresponding failure modes or notes. "**Figure 12**" depicts the results plotted against classifications given in the Aluminum Design Manual, with the data presented on a log-log scale. In the figure, black dots represent 8-inch data points, while orange, green, and yellow lines correspond to detail classifications C, D, and E from the Aluminum Design Manual [30].

Table 3. 8-inch cyclic fatigue test reinforced handhole results.

Stress Range (Mpa)	Specimen #	Handhole Label	Cycle Count	Failure Mode #
17.86	6	A	Cycle Out	N/A
		B	Cycle Out	N/A
24.75	5	A	7,403,758	1
		B	3,418,453	1
31.03	4	A	3,182,311	1
		B	2,102,129	1
38.20	3	A	1,386,613	1
		B	980,523	2
44.33	2	A	476,946	2
		B	760,440	2
50.95	1	A	410,495	2
		B	173,055	1
62.68	7	A	109,194	2
		B	79,489	2

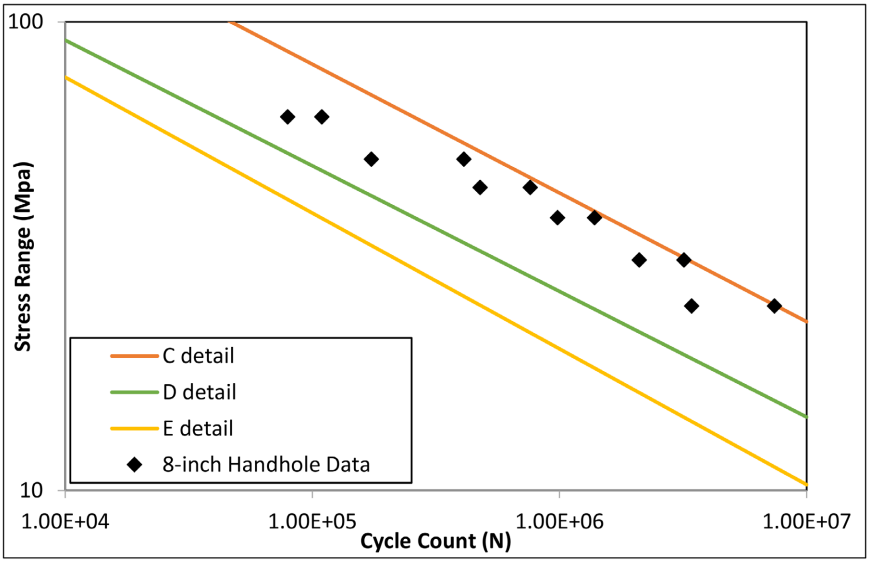

Figure 12. 8-inch cyclic fatigue test reinforced handhole results plotted against detail classifications.

3.2. Finite Element Analysis

The FEA models are illustrated in "**Figures 13-15**", each focusing directly on the handhole, which serves as the central point of the study. "**Figure 13**" depicts the longitudinal local stress field, aligned with the major axis of the experiments, while "**Figure 14**" depicts the transverse local stress field, aligned with the minor axis. "**Figure 15**" depicts the local shear stress field around the handhole. In each figure, the color scale depicts how stresses accumulate around the reinforced handhole, with warmer colors indicating tension and cooler colors indicating compression, with variations in between.

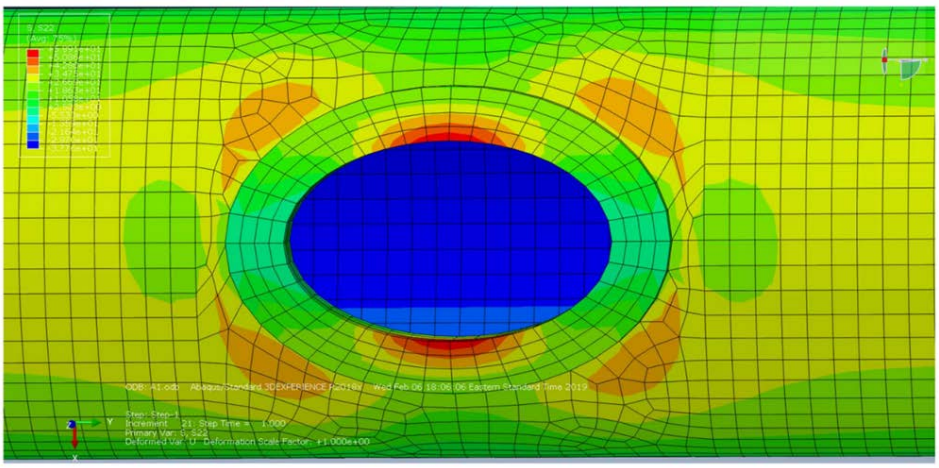

Figure 13. Longitudinal (major axis) local stress field.

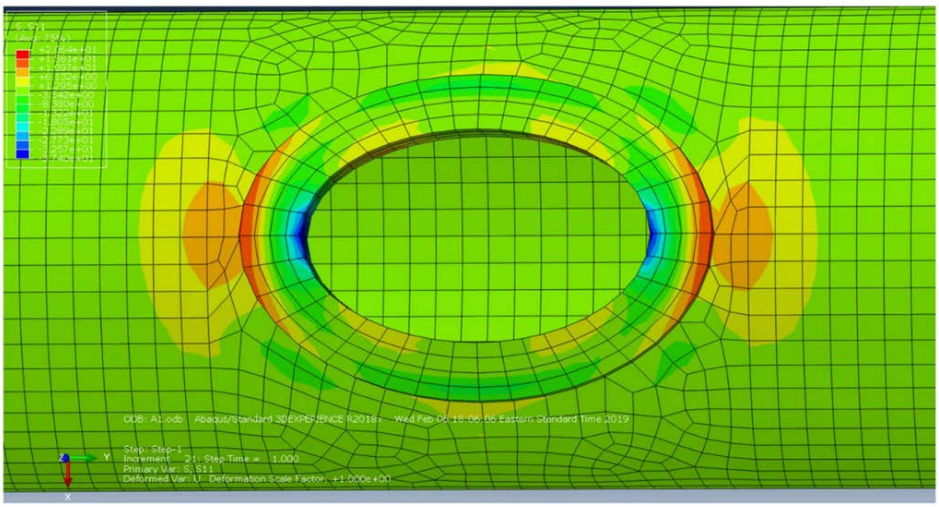

Figure 14. Transverse (minor axis) local stress field.

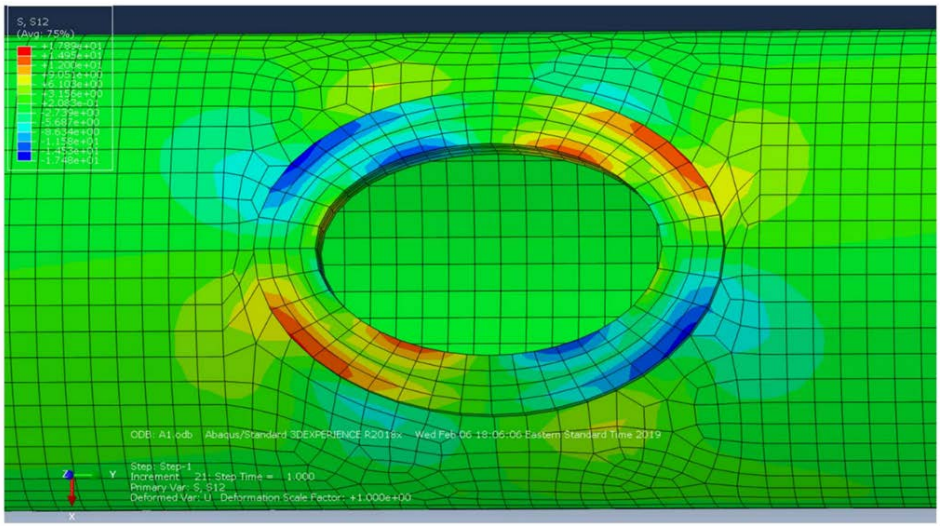

Figure 15. Local shear stress field.

3.3. Statistical Analysis

The power regression statistical analysis of the 8-inch and 10-inch specimens is depicted in "Figure 16" and "Figure 17". These plots were generated by fitting a power trend line to experimental data within each size category (8-inch and 10-inch), yielding an equation. This equation allows determination of stress range values for any cycle count between 100 and 20,000,000 cycles. Each analysis includes the data points, power trend line derived from experimental data, and the corresponding equation the trend lines represent.

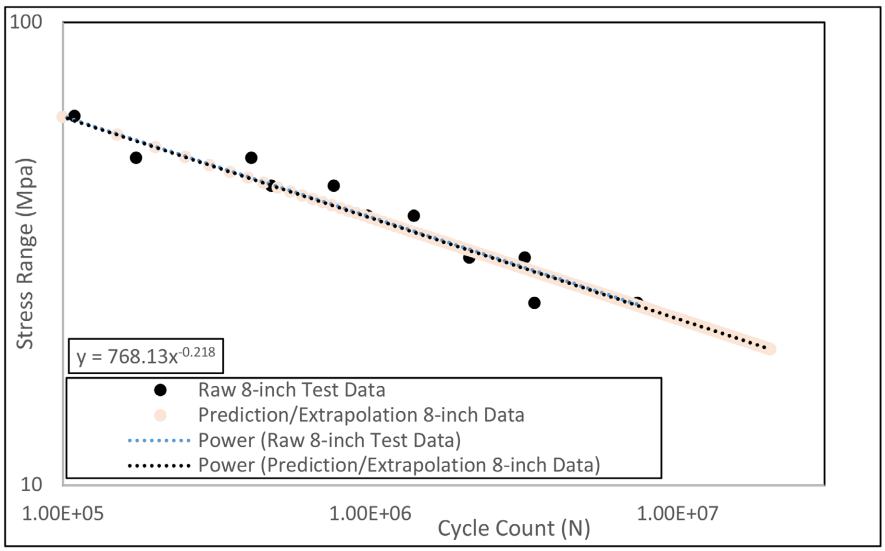

Figure 16. 8-inch diameter specimens power regression statistical analysis.

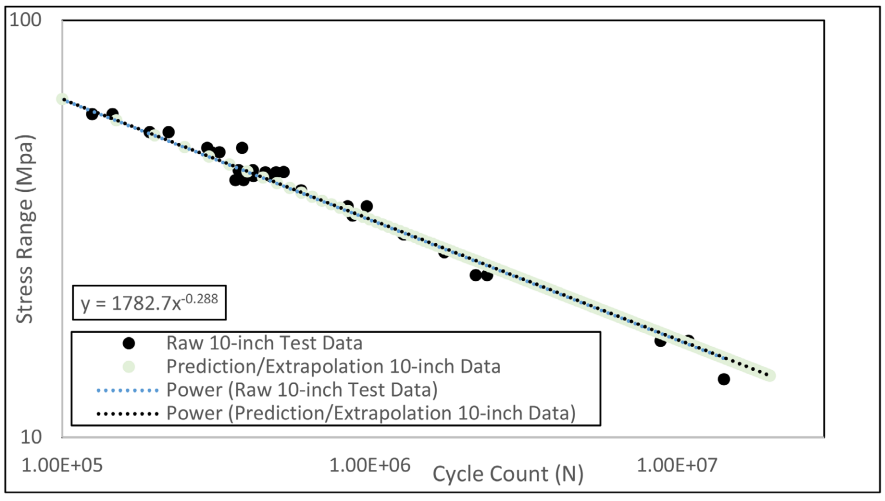

Figure 17. 10-inch diameter specimens power regression statistical analysis.

3.4. Comparison Analysis

The S-N fatigue data for the 8-inch reinforced handholes was plotted alongside the fatigue data for 10-inch handholes from the study conducted by Schlatter

[16], as depicted in "Figure 18". The formatting mirrors that of "Figure 12", with the addition of blue markings indicating the 10-inch dataset. Trendlines were incorporated for both datasets to facilitate comparison.

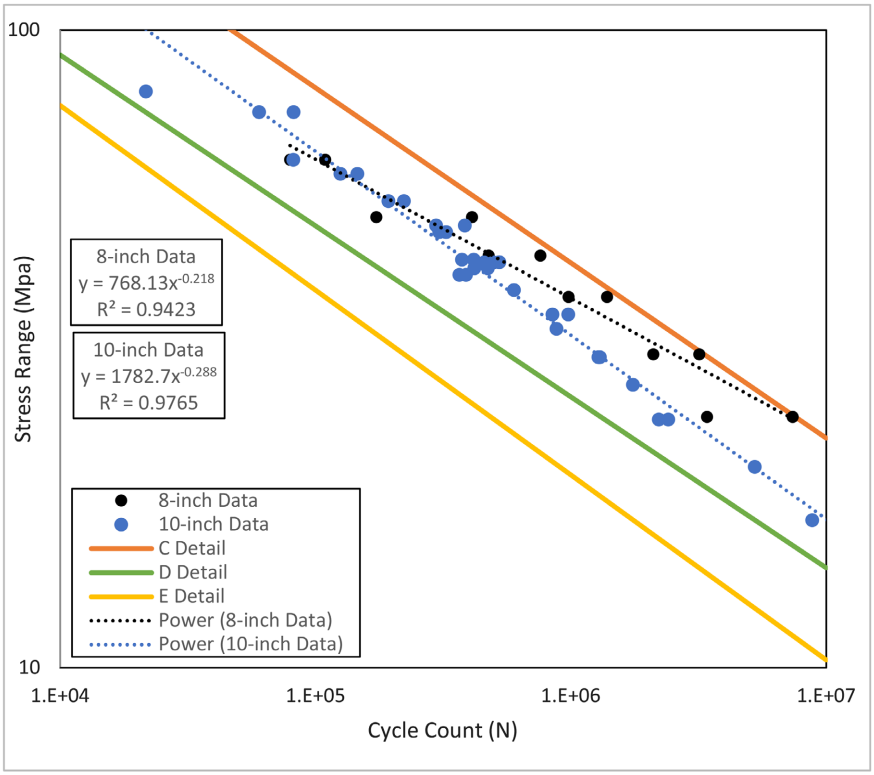

Figure 18. Comparison analysis with 8-inch data plotted with 10-inch data.

4. Summary and Discussion

Cyclic fatigue tests were performed on seven (7) different specimens, each containing 2 reinforced handholes. The study involved two distinct failure modes, plotted S-N curves, finite element analysis (FEA), statistical analysis, and comparison analysis based on the test outcomes. The key findings and observations derived from the testing procedures and subsequent analyses are summarized as follows:

- Test results revealed no predominant failure mode; each mode occurred six times during testing.
- The differentiation of failure modes depended on the stress range applied to the specimen. Lower stress ranges induced failure mode one, while higher stress ranges induced failure mode two. The transition from mode two to mode one occurred around the 38.0 MPa stress range.
- Specimen number 6, cycled at 17.86 Mpa, achieved infinite fatigue life, showing no signs of failure and reaching a cycle count of 20,000,000.
- All test data fell above fatigue detail classification D and below classification C.

- Finite Element Analysis (FEA) in "Figure 13" depicted tensile stresses predominantly along the outer perimeter of the reinforcement, particularly at the 1:00, 4:00, 7:00, and 11:00 positions surrounding the handhole. Additionally, an elevated stress field was observed on the inner side of the reinforcement at the 3:00 and 9:00 positions. The stress concentrations on the outer side correspond to locations where fatigue cracks might develop and progress around the weldment consistent with Failure Mode 1. Conversely, "Figure 14" depicted heightened tensile stresses at the 12:00 and 6:00 positions along the minor axis of the handhole/pole, consistent with Failure Mode 2 under larger stress ranges.
- The FEA highlights that tensile stresses predominantly govern the failure modes. Failure mode one typically experiences final failure in regions coinciding with the largest longitudinal compressional stresses in the pole (depicted in "Figure 13"), while failure mode two experiences rupture at locations coinciding with the largest transverse compressional stresses in the pole (depicted in "Figure 14").
- The power regression analysis revealed a significant inverse relationship: as stress range levels decreased, cycle counts substantially increased towards an apparent infinite fatigue life threshold. Notably, as specimens neared the 20,000,000-cycle mark (deemed the maximum by the research team), the 8-inch diameter specimens exhibited a stress level of approximately 19.67 MPa, which was noticeably higher than the 14.07 MPa observed in the 10-inch specimens.
- Comparison analysis revealed that the 8-inch specimens exhibited a longer fatigue life than their 10-inch counterparts. At larger stress ranges, fatigue life was comparable, while at smaller stress ranges, the smaller specimens demonstrated significantly longer fatigue life, up to 39.0%. The divergence in fatigue life between comparable specimens and those exhibiting longer fatigue life occurred around the 50.0 MPa cycle range.

5. Conclusions

The results of the seven (7) experiments on 8-inch diameter aluminum light poles containing handholes reveal that these handholes are critical areas susceptible to failure within the overall structure. Finite Element Analysis (FEA) corroborated the experimental findings by pinpointing heightened stresses at the location of failure. The 8-inch diameter specimens exhibited a fatigue life that was on average 30.7% longer than the 10-inch diameter counterparts. FEA findings further confirmed heightened stress concentrations around the handhole and its reinforcement. There was a point of "infinite fatigue life" identified between the 24.75 and 17.86 MPa stress ranges. Extrapolation from the statistical analysis showed that this point of infinite fatigue appears to align closely with the 20.00 Mpa stress range. Further experimentation could refine the determination of this threshold. Based on the findings, the research team recommends a fatigue detail classification of D from the ADM when designing and analyzing 8-inch diameter aluminum light poles containing handholes.

Future experimental studies could explore the nuances of various aspect ratios found in handholes, such as a rectangular design measuring 5-inch by 4-inch. Additionally, an avenue for further investigation would involve integrating the light pole base into the testing protocol. While previous research has examined each component separately (handholes [15]-[21] and pole bases [40]), there remains an untapped opportunity to examine their combined effects. Such a study could elucidate which welded aspect of light pole design is more susceptible to failure.

Author Contributions

The work presented in this paper was a part of the master's thesis work [20] of now Dr. Cameron R. Rusnak. He oversaw the project and tasks included the oversight of testing, finite element analysis and data processing. Aya Al-Hamami aided in the analysis procedures and writing. Dr. Craig Menzemer secured funding and served as the project advisor.

Funding

This research received financial support from Hapco Pole Products. The opinions, findings, and conclusions presented in this paper are solely those of the authors and do not represent the views of the sponsor.

Conflicts of Interest

The authors declare that the research was conducted in the absence of any commercial or financial relationships that could be construed as a potential conflict of interest.

References

[1] Nova Pole (2020) The Importance of Effective Street Light Poles/Streed Lighting Poles.

[2] CMI Companies (2023) Why Light Poles Are Important and How You Can Maintain Them.

[3] Hapco (2024) Reinforced Handholes. Online Article, Pole Accessories, Reinforced Handholes, Hapco Pipe Products.

[4] Garlich, M.J. and Thorkildsen, E.T. (2005) Guidelines for the Installation, Inspection, Maintenance and Repair of Structural Supports for Highway Signs, Luminaires, and Traffic Signals. Technical Report Number: FHWA NHI 05-036.

[5] Taplin, G., Sanders, G., Maklary, Z. and Connal, J. (2006) Fatigue Failures of Light Poles. National Academies, Sciences/Engineering/Medicine.

[6] Ireland, B. (2010) The Harder They Fall. MC&M Endeavor Business Media, LLC, Lighting & Control.

[7] Steinbach, P. (2009) Importance of Support-Pole Specification, Inspection. Athletic Business.

[8] Peveto, K. (2010) Fall-Prone Light Poles Used at Southeast Texas Schools. Beau-

mont Enterprise.

[9] GES Tech Group (2014) Light Pole Fatigue Crack Fail. General Engineering Science and Technology Group.

[10] Tsai, L.W. and Alipour, A. (2020) Assessment of Fatigue Life and Reliability of High-Mast Luminaire Structures. *Journal of Constructional Steel Research*, **170**, Article ID: 106066. https://doi.org/10.1016/j.jcsr.2020.106066

[11] Koob, M.J. (2007) Base Connection Retrofits for High Mast Towrs and Pole Luminaries Used for Roadway and Bridge Lighting. *Bridge Structures*, **3**, 67-80. https://doi.org/10.1080/15732480601103747

[12] Roy, S., Park, Y.C., Sause, R., Fisher, J.W. and Kaufmann, E.J. (2011) NCHRP Web-Only Document 176, Cost-Effective Connection Details for Highway Sign, Luminaire, and Traffic Signal Structures. Advanced Technology for Large Structural Systems (ATLSS) Center.

[13] Consolazio, G.R., Johns, K.W. and Dexter, R.J. (1998) Fatigue Performance of Variable Message Sign & Luminaire Support Structures. Volume II—Fatigue Testing and Failure Analysis of Aluminum Luminaire Support Structures. Federal Highway Administration U.S. Department of Transportation, Washinton DC, Report No. FHWA 1998-010.

[14] Oterkus, E., Madenci, E. and Nemeth, M.P. (2005) Stress Analysis of Composite Cylindrical Shells with an Elliptical Cutout. Technical Report, American Institute of Aeronautics and Astronautics. https://doi.org/10.2514/6.2005-1824

[15] Azzam, D. (2006) Fatigue Behavior of High Welded Aluminum Light Pole Support Structures. Master's Thesis, The University of Akron. https://doi.org/10.1061/(ASCE)0733-9445(2006)132:12(1919)

[16] Daneshkhah, A., Schlatter, C., Rusnak, C. and Menzemer, C. (2019) Fatigue Behavior of Reinforced Welded Hand-Holes in Aluminum Light Poles. *Engineering Structures*, **188**, 60-68. https://doi.org/10.1016/j.engstruct.2019.03.013

[17] Schlatter, C. (2017) Fatigue Behavior of the Reinforced Electrical Access Hole in Aluminum Light Support Structures. Master's Thesis, The University of Akron.

[18] Rusnak, C. and Menzemer, C. (2021) Fatigue Behavior of Flush Welded Hand-Holes in Aluminum Light Poles. *Engineering Structures and Materials*, **7**, 465-480. https://doi.org/10.17515/resm2021.248st0122tn

[19] Rusnak, C. and Menzemer, C.C. (2021) Fatigue Behavior of Nonreinforced Hand-Holes in Aluminum Light Poles. *Metals*, **11**, Article 1222. https://doi.org/10.3390/met11081222

[20] Rusnak, C. and Menzemer, C. (2022) Fatigue Behavior of Reinforced Welded Hand-Holes in Aluminum Light Poles with a Change in Detail Geometry. IntechOpen.

[21] Rusnak, C. and Menzemer, C. (2023) Fracture Mechanics, and Its Application in the Fatigue Behavior of Reinforced Welded Hand-Holes in Aluminum Light Poles. *Open Journal of Civil Engineering* (*OJCE*), **13**, 677-694. https://doi.org/10.4236/ojce.2023.134045

[22] Rusnak, C. (2019) Fatigue Behavior in Reinforced Electrical Access Holes in Aluminum Light Support Structures. Master's Thesis, The University of Akron.

[23] Rusnak, C. (2022) Fatigue Behavior in Electrical Access Holes in Aluminum Light Support Structures. Master's Thesis, The University of Akron.

[24] Hoeppner, D.W. and Krupp, W.E. (1974) Prediction of Component Life by Appli-

cation of Fatigue Crack Growth Knowledge. *Engineering Fracture Mechanics*, **6**, 47-62. https://doi.org/10.1016/0013-7944(74)90046-0

[25] Fatemi, A. and Yang, L. (1998) Cumulative Fatigue Damage and Life Prediction Theories: A Survey of the State of the Art for Homogeneous Materials. *International Journal of Fatigue*, **20**, 9-34. https://doi.org/10.1016/S0142-1123(97)00081-9

[26] Carpinteri, A., Spagnoli, A. and Vantadori, A. (2009) Size Effect in Finite-Life Fatigue of Metals. Department of Civil-Environmental Engineering & Architecture, University of Parma.

[27] (1995) Access NCBI through the World Wide Web (WWW). *Molecular Biotechnology*, **3**, 75. https://doi.org/10.1007/BF02821338

[28] Li, J. (2008) Research of Knowledge Discovery Based on Information Entropy Petri Net Model. *Journal of Computer Applications*, **28**, 1649-1651. https://doi.org/10.3724/SP.J.1087.2008.01649

[29] Ahmed Marzouk, O. (2017) Case Studies of Statistical Analysis in Engineering. *International Journal of Statistical Distributions and Applications*, **3**, 32-37. https://doi.org/10.11648/j.ijsd.20170303.12

[30] ADM (2015) Aluminum Design Manual 2015. The Aluminum Association.

[31] Minnick, W.H. and Mosman, J. (2023) Gas Metal Arc Welding Procedures for Aluminum. In: Minnick, W.H. and Mosman, J., Eds., *GMAW/FCAW Handbook* (2*nd Edition*), Goodheart-Willcox, 93-102.

[32] Matweb (2024) Aluminum 6063. Matweb Material Property Data, Online Database.

[33] Matweb (2024) Aluminum A356-T6. Matweb Material Property Data, Online Database.

[34] AlcoTec (2024) Alloy 4043 Weld Data Sheet. AloTec Wire Corporation, Data Sheet.

[35] Hapco (2015) Specifications, Hapco Specifications Advantage. Hapco Pipe Products.

[36] Miner, M.M. (1945) Cumulative Damage in Fatigue. *The American Society of Mechanical Engineers*, *Applied Mechanics*, **12**, 159-164. https://doi.org/10.1115/1.4009458

[37] Uherek, F.C. (2023) What Is Miner's Rule? Rexnord.

[38] American Society for Testing and Materials (2017) Standard Practices for Cycle Counting in Fatigue Analysis. ASTM E1049-85.

[39] Metal Fatigue Life Prediction (2024) Rainflow Counting.

[40] Daneshkhah, A. and Menzemer, C. (2019) A Finite Element Study of Welded Aluminum Shoe-Base Light Pole Details. *Engineering Structures*, **198**, Article ID: 109506. https://doi.org/10.1016/j.engstruct.2019.109506